Pre-print

Liao, J., Malusà, M. G., Zhao, L., Baldwin, S. L., Fitzgerald, P. G., & Gerya, T. (2018)

Divergent plate motion drives rapid exhumation of (ultra) high pressure rocks.

Earth and Planetary Science Letters, 491, 67-80.

https://doi.org/10.1016/j.epsl.2018.03.024

Divergent plate motion drives rapid exhumation of (ultra)high pressure rocks

Jie Liao*[1], Marco G. Malusà *[2], Liang Zhao[3], Suzanne L. Baldwin[4], Paul G. Fitzgerald[4], Taras Gerya[1]

[1]Geophysical Fluid Dynamics, Institute of Geophysics, ETH Zurich, Switzerland

[2]Department of Earth and Environmental Sciences, University of Milano-Bicocca, Milan, Italy

[3]State Key Laboratory of Lithospheric Evolution, Institute of Geology and Geophysics, Chinese Academy of Sciences, Beijing, China

[4]Department of Earth Sciences, Syracuse University, Syracuse, New York, USA

Authors for correspondence: Jie Liao (jie.liao@erdw.ethz.ch); Marco G. Malusà (marco.malusa@unimib.it)

Abstract

Exhumation of (ultra)high pressure [(U)HP] rocks by upper-plate divergent motion above an unbroken slab, first proposed in the Western Alps, has never been tested by numerical methods. We present 2D thermo-mechanical models incorporating subduction of a thinned continental margin beneath either a continental or oceanic upper plate, followed by upper-plate divergent motion away from the lower plate. Results demonstrate how divergent plate motion may trigger rapid exhumation of large volumes of (U)HP rocks directly to the Earth's surface, without the need for significant overburden removal by erosion. Model exhumation paths are fully consistent with natural examples for a wide range of upper-plate divergence rates. Exhumation rates are systematically higher than the divergent rate imposed to the upper plate, and the modeled size of exhumed (U)HP domes is invariant for different rates of upper-plate divergence. Major variations are instead predicted at depth for differing model scenarios, as larger amounts of divergent motion may allow mantle-wedge exhumation to shallow depth under the exhuming domes. The transient temperature increase, due to ascent of mantle-wedge material in the subduction channel, has a limited effect on exhumed continental (U)HP rocks already at the surface. We test two examples, the Cenozoic (U)HP terranes of the Western Alps (continental upper plate) and eastern Papua New Guinea (oceanic upper plate). The good fit between model predictions and the geologic record in these terranes encourages the application of these models globally to pre-Cenozoic (U)HP terranes where the geologic record of exhumation is only partly preserved.

Keywords: upper-plate divergent motion; (U)HP rock exhumation; mantle-wedge exhumation; Western Alps; eastern Papua New Guinea

1. Introduction

Exhumed slivers of ultra-high pressure (UHP) rocks of continental origin have been found in many localities since their discovery in the 1980s (Fig. 1) (e.g., Chopin, 2003; Guillot et al., 2009). They provide compelling evidence of continental subduction, which is also revealed in seismic sections (Roecker, 1982; Zhao et al., 2015). Exhumation of these rocks to the surface and the processes responsible still remain a matter of debate (e.g., Hacker and Gerya, 2013; Ducea, 2016, and references therein). Quantitative insights are provided by thermo-mechanical numerical models (Beaumont et al., 2001; Li et al., 2011), most of which rely on synconvergent exhumation. These models typically predict the buoyant rapid rise of relatively small (U)HP rock volumes to the base of the crust, followed by slower transcrustal exhumation (e.g., Yamato et al., 2008; Butler et al., 2013), but significant erosion is also required to exhume these rocks to the surface. Models of synconvergent exhumation are therefore inadequate to explain (U)HP terranes that have reached the Earth's surface rapidly, and within a tectonic scenario characterized by negligible erosion during exhumation, such as the Western Alps and eastern Papua New Guinea (PNG) (e.g., Baldwin et al. 2012; Malusà et al., 2015) (Fig. 1). Recent models of trans-mantle diapiric exhumation applied to eastern PNG (Ellis et al., 2011) are in conflict with part of the geologic and geophysical record (e.g., Petersen and Buck, 2015; Abers et al., 2016). Alternative hypotheses for (U)HP exhumation that consider divergence within the subduction zone have been proposed since the early 1990s (e.g., Andersen et al., 1991). These include subduction inversion (Webb et al. 2008), slab eduction after breakoff (Petersen and Buck, 2015), slab rollback (Brun and Faccenna, 2008), and subduction-wedge exhumation triggered by upper-plate divergent motion above an unbroken slab (Malusà et al., 2011). In the eduction model of Andersen et al. (1991), significant erosion of ~30 km, in combination with tectonic extension, is required to exhume the deepest rocks exposed in the Western Gneiss Region. Slab rollback may explain the multiple exhumation pulses of blueschists in the Mediterranean (Brun and Faccenna, 2008), but this mechanism is not documented for higher pressure belts such as the Western Alps (Malusà et al., 2015). (U)HP rock exhumation triggered by upper-plate divergent motion above an unbroken slab, first proposed in the Western Alps (Malusà et al., 2011), is potentially consistent with the geologic record of several (U)HP belts worldwide, including eastern PNG where (U)HP exhumation is active. However, the ability of this mechanism to exhume large volumes of (U)HP rocks without the requirement of significant erosion, and in the absence of slab breakoff, has never been investigated using numerical methods.

The objective of this paper is to evaluate (U)HP rock exhumation due to upper-plate divergent motion above an unbroken slab using a 2D thermo-mechanical numerical model. Results indicate that upper-plate divergent motion can trigger rapid exhumation of large volumes of (U)HP rocks directly to the Earth's surface, without the requirement of significant overburden removal by erosion. This mechanism produces the main tectonic structures observed in most continental (U)HP belts, and may provide insight for the exhumation of many (U)HP terranes worldwide.

2. Rationale and geodynamic framework

Orogenic belts associated with former subduction of continental rocks may preserve an accurate geologic record of (U)HP rock exhumation. The Paleogene Western Alps in southern Europe and the Neogene D'Entrecasteaux Islands of eastern PNG (Fig. 1) provide two examples of terranes that include (U)HP rocks of continental origin (Compagnoni, 2003; Baldwin et al., 2012). The Western Alps, also include (U)HP metaophiolites (e.g., Groppo et al., 2009). We focus our attention on the exhumation of continental (U)HP rocks, which is invariably very rapid in these two examples (Rubatto and Hermann, 2001; Baldwin et al., 2004). In our numerical models, we consider subduction beneath a continental upper plate, as observed in the Western Alps, and beneath an oceanic upper plate, as observed in eastern PNG (Fig. 1). While a perfect fit of the 2-D models with natural examples should not be expected due to the influence of trench-parallel plate motion (e.g., Baldwin et al., 2012; Malusà et al., 2015), the 2-D models reproduce the main geologic features observed in both (U)HP belts. These include:

a) Continental (U)HP rocks are exhumed within tectonic domes bounded by extensional shear zones (e.g., Blake and Jayko, 1990; Hill, 1994). These domes are located at the rear of an accretionary wedge that includes lower-pressure metamorphic rocks (Malusà et al., 2011; Webb et al., 2014) (Fig. 1).

b) Both in the Western Alps and eastern PNG, (U)HP rock exhumation takes place when formation of the lower-pressure frontal wedge is complete. Available geologic constraints suggest that continental eclogites do not stall in the mid-upper crust before final exhumation, as predicted for synconvergent exhumation models, but are rapidly exhumed to the upper crust, reaching close to sea level in a few million years (e.g., Baldwin et al., 2004; Malusà et al., 2015).

c) Continental (U)HP units show either lithologic mixing at the outcrop scale (Baldwin et al., 2008), or comprise coherent crust slivers preserving in places the pre-subduction relationships between different lithologies (e.g., Compagnoni and Rolfo, 2003). The (U)HP metaophiolites enveloping the continental (U)HP domes of the Western Alps (e.g., the Viso metaophiolites) are pervasively deformed, and include mixed lithologies and tectonic mélanges (e.g., Schwartz et al., 2000). However, in the Western Alps a metamorphic field gradient can be recognized at the scale of the whole plate-boundary zone (Compagnoni, 2003).

d) The volume of syn-exhumation sediments is generally negligible (Malusà et al., 2011; Fitz and Mann, 2013), with some sediments deposited unconformably on top of the accretionary wedge (Fig. 1). This suggests that the contribution of erosion to (U)HP rock exhumation is minor (Malusà e al., 2015).

e) Continental (U)HP domes may occur above exhumed portions of the mantle wedge, as suggested in the Western Alps by recent geophysical experiments (Solarino et al., 2018). The occurrence of anomalously deep earthquakes (Abers et al., 2016; Malusà et al., 2017) may be supportive of low geothermal gradients persisting in the upper plate during and after (U)HP rock exhumation (Malusà et al., 2017). Magmatism post-dates (U)HP exhumation, and may only occur in case of protracted post-exhumation tectonic extension (e.g., Baldwin et al., 2012) (Fig. 1).

3. The Western Alps reference case

In the (U)HP belt of the Western Alps (Fig. 2), the geologic record listed above is preserved in full. The Western Alps formed during Late Cretaceous to Paleogene subduction of the Tethyan ocean and adjoined European paleomargin beneath the Adriatic continental microplate (Compagnoni, 2003; Zhao et al., 2016, and references therein). The Alpine wedge includes three main tectonic domains (Fig. 2a): (i) a Cretaceous accretionary wedge that was already part of the Adriatic upper plate during Paleogene subduction and exhumation of (U)HP rocks; (ii) a doubly-vergent Paleogene Frontal wedge located close to the European mainland, consisting of blueschist-to-(sub)greenschist facies rocks derived from the European paleomargin (Br in Fig. 2a), and metasediments and minor ophiolites derived from the Tethyan ocean (SL, EU and Va in Fig. 2a); (iii) an Eocene Eclogite belt consisting of (U)HP continental crust domes of European derivation (DM, GP and MR in Fig. 2a), tectonically enveloped by (U)HP metaophiolites. The continental units of the Eclogite belt reached peak pressure in the subduction channel at ~35 Ma (e.g., Rubatto and Hermann, 2001). They were rapidly exhumed to the Earth's surface at rates of 1-3 cm/yr by 32 Ma (Fig. 2b), when they were unconformably covered by corals and syntectonic sediments (Malusà et al., 2015). These sediments are still preserved in the southern part of the Eclogite belt (Molare Fm, green star in Figs. 1c and 2b) because subsequent erosional exhumation was minor in this part of the belt compared to the northern part (Malusà et al., 2005). The volume of syn-exhumation clastic detritus preserved in sedimentary basins around the Alps (Fig. 2b) is much less than predicted by numerical models of synconvergent exhumation, whereas the amount of exhumed (U)HP rocks is much greater. (U)HP rocks, floored in places by serpentinized mantle-wedge peridotites (e.g., under the Dora-Maira dome), represent in fact one third of the total width of the Alpine metamorphic belt (Fig. 2a). These features are interpreted to result from a kinematic change along the Adria-Europe plate boundary zone in the Eocene (Dewey et al., 1989), possibly leading to a divergent component of relative plate motion between the European slab and the Adriatic upper plate (Malusà et al., 2011). The component of trench-normal divergence has been suggested as sufficient to make space for the exhumation of (U)HP continental rocks on the upper plate side of the orogen, without requiring overburden removal by significant erosion. We present results of numerical models that test this hypothesis.

4. Methods

4.1 Numerical method

We use a 2D thermo-mechanical coupled numerical code (Gerya and Yuen, 2003a) based on finite-differences and marker-in-cell techniques to solve the mass, momentum and energy conservation equations in a fully staggered grid assuming an incompressible media (see details in Supplementary Methods). Governing equations are solved coupled with rheology laws. Visco-plastic rheology is employed in our models, where viscous rheology is largely dominated by dislocation creep, and plastic rheology is described by Mohr-Coulomb failure. The transition from viscous rheology to plastic rheology is determined by the Drucker-Prager yield criterion. Peierls creep, which takes over from dislocation creep at high stress and mainly influences the strength of the uppermost mantle, is also implemented. Effective viscosity of rocks in our model is thus constrained by all these rheology laws (see Liao and Gerya, 2014 for details). Erosion and sedimentation at the surface is implemented by solving the diffusion equation on the Eulerian nodes at each time step (Gerya and Yuen, 2003b). Our erosion/sedimentation model uses gross-scale erosion/sedimentation rates which are independent of local elevation and topography (Burov and Cloetingh, 1997). The constant and moderate rates of erosion (0.315 mm/yr) and sedimentation (0.0315 mm/yr) fall within naturally observed ranges.

4.2 Model setup

Based on available geological and geophysical constraints from the Western Alps (Fig. 2a), we designed a self-consistent subduction-driven reference model with a physical dimension of 2000 km by 680 km. The numerical resolution is 626 by 382 nodes, with denser grids in the middle and upper part of the model domain. Two continental plates separated by oceanic lithosphere are imposed in the model box. Both continental plates consist of upper crust, lower crust, and mantle lithosphere underlain by asthenospheric mantle. Oceanic lithosphere has an initial cold slab nose that is used, together with a weak zone (k in Fig. 3), to trigger spontaneous subduction. A Cretaceous wedge formed by metamorphic rocks (f in Fig. 3) and a precursor frontal wedge formed by accreted sediments (e in Fig. 3) are prescribed along the trench in agreement with geologic constraints from the Western Alps (Malusà et al., 2015). Several tracers are imposed on the normal and thinned continental crust of the lower plate, in order to trace the depth-time paths of exhumed rocks.

The velocity boundary condition is free slip for all boundaries in the model. With the imposed 20-km thick sticky air, the upper surface of the solid portion of the model behaves as a free surface (e.g., Crameri et al., 2011), since shear stress along the surface is minimized by the large viscosity contrast between the sticky air and rocks. Subduction is driven solely by gravitational instability. After 20 Myr, a constant divergent velocity (2 cm/yr in the reference model shown in Fig. 3) is prescribed to the lithosphere (from Y=20 km to Y=120 km) of the upper plate at X=1600 km. Since our reference model does not include the subduction initiation process (e.g., Nikolaeva et al., 2010), the subduction duration is relatively short. However, we also tested this setup for longer subduction durations of 30 Myr and 40 Myr, even though we are aware that such a variability is not sufficient to represent all of the potential natural cases. The early stage of subduction in our reference model is required to subduct rocks to depths consistent with petrologic observations, but in this paper, we only explore in detail the evolution after the onset of divergent motion (t_D). We analyze the model evolution, the evolving temperature, viscosity and velocity fields during subduction and exhumation (Figs. 4, 5), as well as the impact of variable divergence rates prescribed to the upper plate (1 to 5 cm/yr). We examine the P-t paths recorded by different tracers for variable divergence rates, and the potential impact of tectonic overpressure and late erosional exhumation (Fig. 6). We also evaluate the areal extent of exhumed (U)HP rocks (e in Fig. 6a) compared to the total width of the metamorphic belt (w in Fig. 6a). We calculate the sediment volume produced during (U)HP rock exhumation (Fig. 7), which is normalized to the sediment volume calculated at time t_D along a section above the exhuming (U)HP rocks (see section svc – “sediment volume calculation” in Fig. 6a). Model results are compared with observations from natural cases. Because the upper plate type (continental vs oceanic) could also be important in controlling exhumation processes during upper-plate divergent motion, the reference experiment with divergent velocity of 2 cm/yr is also performed by considering an oceanic upper plate (Fig. 8), as is relevant in the case of the Papuan (U)HP terrane.

5. Model results

5.1. Evolution of the reference model (upper plate is continental)

The numerical evolution of the reference model described in section 4 is shown in Figures 4 and 5. In this model, oceanic subduction initiates spontaneously driven by the cold slab, which then rolls back gradually. The normal (~35 km thick) continental crust of the lower plate is dragged to ~40 km depth, and is then exhumed within a doubly-vergent accretionary wedge prior to the onset of upper-plate divergent motion (triangles in Fig. 4a, see also the inset of Fig. 5b). The thinned continental crust exposed on the leading edge of the former passive margin experiences deeper subduction within the subduction channel (circles 1 to 8 in Fig. 4a). Before the onset of upper-plate divergent motion, the upper plate is coupled with the subducted lower plate (Fig. 5a,b). The horizontal motion of the upper plate towards the lower plate is faster during initial oceanic subduction, and progressively slows down during continental subduction. After the onset of upper-plate divergent motion, the dynamics of subduction changes dramatically (Fig. 5c). The asthenospheric mantle flows upward, towards the subduction channel to fill the accommodation space created by the upper-plate divergent motion. The subducting plate slows down significantly (Fig. 5c) and the slab dip angle decreases, as illustrated by a Moho rebound of ~10 km relative to the Moho depth before time t_D (red dashed line in Fig. 4b,c). The upper plate decouples from the lower plate and moves away, continuing to generate accommodation space along the subduction zone.

This dynamic scenario facilitates the extremely fast exhumation of continental (U)HP rocks previously dragged into the subduction channel. Continental (U)HP rocks are exhumed very rapidly, reaching the Earth's surface in ~3 Myr (Fig. 4b,c), to form a dome ~30 km across at the rear of the low-grade accretionary wedge (Fig. 4c). This low-grade wedge includes continental crust rocks exhumed in the rear part of the wedge (c in Fig. 6a), and slivers of oceanic crust (b), oceanic sediments (e) and serpentinites (k, l) forming both the frontal part of the wedge and ophiolitic nappes on top of the low-grade continental rocks. Within the exhumed (U)HP dome, tracers have the same order imposed during model setup along the continental margin (cf. Fig. 3), which suggests a relative internal coherence of the (U)HP terrane. These tracers, in the light of the maximum pressure recorded and of their final position, may define a metamorphic field gradient. By contrast, the ophiolitic envelope of the dome consists of extremely well-mixed serpentinites and oceanic sediments (Fig. 6a).

During subduction, lithologies on top of the downgoing slab evolve due to interaction between slab-released fluids and the mantle wedge, forming serpentinized peridotites (l) and hydrothermally altered mantle rocks more generally (m). After the onset of upper-plate divergent motion, these buoyant lithologies rise through the subduction channel, forming a plug that fills the accommodation space below the exhuming continental (U)HP rocks (Fig. 4b). As upper-plate divergence continues, these mantle-wedge rocks are finally emplaced at relatively shallow depths beneath the continental (U)HP dome (Fig. 4c). The rising mantle-wedge material causes a transient rapid temperature increase in the subduction channel, which has limited effect on continental (U)HP rocks that are already exhumed to shallower crustal levels. Note that temperatures in the lithospheric mantle of the upper plate remain low following the onset of upper-plate divergent motion (Fig. 5d). Dry mantle peridotites may be brittlely deformed even at depths >60 km and far away from the former subduction thrust (Fig. 5d).

As upper-plate divergence proceeds, the relatively short stage of (U)HP rock exhumation is followed by a rifting stage associated with the rise of asthenospheric mantle (Fig. 4d,e). During this stage, temperatures progressively increase both within the (U)HP dome and at the base of the low-grade accretionary wedge. The low-grade wedge is progressively extended, its distance from the exhumed (U)HP dome progressively increases, and the resulting accommodation zone is filled by exhumed mantle-wedge serpentinites (l) and hydrothermally altered peridotites (m). Tectonic extension, during the rifting stage, is largely accommodated not only on the lower-plate side of the (U)HP dome, but also on the upper-plate side, where decompression melting (p) eventually induces magmatism. The lithospheric mantle of the upper plate remains relatively cold.

5.2. Exhumation rate, size of exhumed (U)HP terranes, and role of erosion

Figure 6b compares the pressure-time exhumation path for tracers 1 to 8, representative of continental crust slivers that have reached mantle depths during subduction. Deviations from lithostatic pressure, during the final stages of burial and subsequent exhumation, are shown in the right panel of Fig. 6b for tracer 8, which approaches the coesite stability field. Because this diagram shows that deviations due to tectonic overpressure are minor during upper-plate divergent motion, metamorphic pressures are expected to provide a good indication of maximum burial experienced by rocks in the subduction channel. In the reference model (divergence rate of 2 cm/yr), tracers 1 to 8 synchronously record rapid decompression starting from time t_D (Fig. 6b). These tracers do not stall in the mid-upper crust as predicted by synconvergent exhumation models (grey dashed lines in Fig. 6b), but are immediately exhumed from mantle depths (~80 km for tracer 8) to the uppermost crust. Tracer 3 is directly exhumed from ~70 km depth to the Earth's surface in ~3 Myr, whereas other tracers may require further erosional exhumation before final exposure to the Earth's surface (Fig. 6a). In the case of faster upper-plate divergent motion (3 to 5 cm/yr in Fig. 6c), the slopes of modeled exhumation paths are still invariably very steep (i.e., indicative of rapid exhumation). For slower upper-plate divergent motion (1 cm/yr in Fig. 6c), exhumation paths are less steep, and similar to the paths predicted by synconvergent exhumation models.

The exhumation rate of (U)HP rocks scales with the rate of divergence of the upper plate (Fig. 7a). The modeled highest divergence rate of 5 cm/yr has the highest average exhumation rate (~5.1 cm/yr) and the highest initial exhumation rate. The slowest modeled divergence rate (1 cm/yr) has the slowest average exhumation rate (2.2 cm/yr) and also the slowest initial exhumation, but the rate of exhumation persists at a slightly higher rate for longer durations. Both maximum and average exhumation rates are systematically higher than the divergent rate imposed to the upper plate, due to buoyancy of the (U)HP rocks. As the divergence rate increases, the difference between exhumation and plate-motion rates asymptotically decreases. A prescribed divergence rate of 2 cm/yr, in the reference model of Fig. 4, corresponds to an average exhumation rate of ~3.2 cm/yr, and to a maximum exhumation rate >3.5 cm/yr, which is predicted ~1 Myr following the onset of upper-plate divergent motion (Fig. 7a).

Figure 7b shows the normalized volume of clastic detritus eroded from the accretionary wedge during (U)HP rock exhumation. The sediment volume calculated in the model is normalized to the initial volume calculated along the same section at time t_D. Values <1 indicate that the accretionary wedge undergoes erosion during (U)HP rock exhumation, whereas values >1 indicate active sedimentation. The normalized sediment volume for different rates of upper-plate divergent motion is invariably >1, which indicates that the contribution of erosion to (U)HP rock exhumation is negligible. In addition, another important observation is that the size of exhumed (U)HP rocks, normalized to the total width of the metamorphic belt, does not vary significantly with varying rate of divergence (Fig. 7c). Calculated e/w ratios, where "e" is the width of exhumed eclogitic units and "w" is the width of the whole metamorphic belt, are around 0.33. This ratio is much greater than the ratio predicted by numerical models of synconvergent exhumation (e/w = 0.1; Butler et al., 2013), which suggests that upper-plate divergent motion is a more effective mechanism of (U)HP rock exhumation for larger semi-coherent (U)HP terranes.

5.3. Model evolution incorporating an oceanic upper plate

When the upper plate is oceanic, the results are actually very similar to when it is continental (Fig. 8), which suggests that the upper-plate composition has minor impact on the (U)HP exhumation stage. Continentally derived (U)HP rocks are rapidly exhumed in the subduction channel and form a tectonic dome, ~30 km in size, at the rear of a low-grade wedge that was shaped prior to the onset of upper-plate divergent motion.

Overall, for this model, pressure-time paths indicate rapid decompression from mantle depths (~90 km for tracer 6) to the uppermost crust. (U)HP exhumation is delayed by 1-2 Myr compared to the model of Fig. 4, due to the different rheology of the upper plate. Nevertheless (U)HP exhumation is completed in 3-4 Myr following the onset of upper-plate divergent motion (Fig. 8e). A very important observation is that the continental (U)HP dome does not include an envelope of (U)HP metaophiolites (Fig. 8b), but rather is structurally juxtaposed against oceanic crust of the upper plate (f), very-low-grade oceanic crust of the lower plate (b), and overlying oceanic sediments (e).

The upper plate composition has a greater impact on the model evolution during the subsequent rifting stage (Fig. 8 c,d). For an oceanic upper plate model, compared to the continental upper plate model, deformation on the upper-plate side of the dome is minor, and tectonic extension is more focused in the region between the (U)HP dome and the low-grade wedge, where mantle-wedge serpentinites (l) and lower crust rocks (d) are exhumed. For an oceanic upper plate model, decompression melting (p) is predicted to occur beneath the (U)HP dome (Fig. 8d). In the time frame shown in Fig. 8d, the lithosphere-asthenosphere boundary is near-horizontal beneath the exhumed (U)HP dome, at ~20 km depth. Although the (U)HP rocks were exhumed from within the subduction channel, after the rifting stage they reside directly on top of mantle rocks. Geothermal gradients predicted in the oceanic upper plate model are higher under the dome than in the stretched low-grade accretionary wedge. On the upper-plate side of the dome, a sharp near-vertical boundary within the mantle is predicted, to ~50 km depth, marking the rising asthenosphere and the colder lithospheric mantle of the upper plate. In the upper-plate mantle, relatively low temperatures, consistent with brittle failure in dry mantle peridotite, are possibly found down to depths exceeding 80 km.

6. Comparison with natural examples

6.1. (U)HP rock exhumation in the Western Alps

The reference model with an upper continental plate reproduces most of the geologic observations documented in the Western Alps. There (U)HP rocks of the Eclogite belt are exposed in tectonic domes of ~30 km in size, representing one third of the total width of the Alpine metamorphic wedge (Fig. 2a). The size of modeled exhumed (U)HP rocks is consistent with those observed in the Western Alps (e/w = 0.33, green dashed line in Fig. 7c), irrespective of the prescribed rate of upper-plate divergence. Pressure-time paths calculated in the models are consistent with exhumation paths reconstructed from petrologic and geochronologic data (dark blue area in Figs. 2b and 6b), for the entire range of upper-plate divergence rates between 2 and 5 cm/yr (Fig. 6b). Both in nature and the model, (U)HP rock exhumation takes place when rocks of the low-grade frontal wedge are already exhumed (Figs. 2b and 4). Importantly, some of the (U)HP rocks are exhumed directly to the Earth's surface (tracer 3 in Fig. 6b), and the model exhumation timing is consistent with that in the Western Alps, where the biostratigraphic age of sedimentary rocks unconformably deposited on top of the (U)HP rocks of the Eclogite belt (Molare Fm, green star in Fig. 5b) tightly constrain when (U)HP rocks arrived at the surface. Note that all of the tracers in the model are exhumed rapidly without stalling in the mid-upper crust, and that the exhumation process takes place without a substantial contribution of erosion (Fig. 7b). This result agrees well with the stratigraphic record preserved in sedimentary basins throughout the Alps (Fig. 2b) (Malusà et al., 2011).

The distribution of tracers after exhumation (Fig. 6a), similar to the order imposed during model setup (cf. Fig. 3), suggests a relative internal coherence of exhumed (U)HP units, which may explain the local preservation of pre-subduction relationships between different lithologies (e.g., Compagnoni and Rolfo, 2003). On the other hand, the extreme lithologic mixing characterizing the ophiolitic envelope of the (U)HP domes (e.g., Schwartz et al., 2000) is also successfully reproduced by the model (Fig. 6a). The model distribution of low-grade continental rocks, oceanic metasediments and serpentinites within the Frontal wedge (Fig. 6a) also replicates what is mapped in the Western Alps. The wider exposure of mapped low-grade continental units (Br in Fig. 2a) in the northern part of the Frontal wedge of the Western Alps would be favoured by a deeper level of erosion after the (U)HP exhumation stage, which is in agreement with low-temperature thermochronology studies (e.g., Malusà et al., 2005) (Fig. 2a).

6.2. Mantle-wedge exhumation in the Western Alps

That the size of exhumed domes is independent of the prescribed rate of upper-plate divergent motion is of primary importance. It explains why the (U)HP domes in the Western Alps are about the same size from the north to the south (MR, GP and DM in Fig. 2a), in spite of the southward increasing divergence rate which results from the geometry and kinematics of the Cenozoic Adria-Europe plate boundary (e.g., Solarino et al., 2018). Different time frames (Fig. 4) describe different steps of (U)HP rock exhumation, as well as different segments of the Western Alps belt characterized by varying amounts of upper-plate divergence before subsequent tectonic shortening (Malusà et al., 2015). From this perspective, the snapshot at t_D + 3 Myr (Fig. 4c) may be representative of the evolution of an Alpine transect across the Gran Paradiso dome (GP in Fig. 2a). The snapshot at t_D + 5 Myr (Fig. 4d) is instead more representative of a transect across the Dora-Maira dome (DM in Fig. 2a), where divergence was greater. If the model sequence successfully replicates the natural geologic progression, the relatively similar structure displayed by different (U)HP domes along the strike of the Alpine orogen may be associated with remarkably different structures at depth. As shown in Fig. 4d, the amount of upper-plate divergence along the Dora-Maira cross-section may result in exhumation of mantle-wedge serpentinites at depths of 15-20 km beneath the dome of (U)HP continental crust. Recent geophysical transects

(Malusà et al., 2017; Solarino et al., 2018) suggest that mantle-wedge serpentinites may be present beneath the Dora-Maira, from depths of ~10 to >40 km corresponding to the eclogitized lower crust of the European plate. When late erosional exhumation is taken into account (Fig. 6a), model predictions are remarkably consistent with geologic observations.

6.3. Thermal evolution after (U)HP rock exhumation

According to our numerical models, rising mantle-wedge material causes a transient rapid temperature increase in the subduction channel. Such a temperature increase may not however completely obliterate the metamorphic record of (U)HP rock exhumation, because continental (U)HP rocks are already exhumed to shallower crustal levels. However, the temperature increase may induce partial isotopic resetting and late-stage partial melting and recrystallization. These findings are consistent with coesite preservation in the Dora-Maira (Compagnoni and Rolfo, 2003; Chopin, 2003), and with the petrologic evidence of late-stage heating following rapid decompression in the main (U)HP continental units of the Western Alps (Compagnoni, 2003).

Model predictions concerning the thermal structure of the upper-plate lithospheric mantle, which may remain relatively cold after mantle-wedge exhumation, are confirmed by the occurrence of anomalously deep earthquakes recorded in the hinterland of the Western Alps. These earthquakes occur ~50 km away from the mountain belt at depths to ~75 km (Malusà et al., 2017) (Fig. 2a). Note that the Western Alps never reached the stage of Fig. 4e. However, the stage shown at Fig. 4e may be characteristic of other (U)HP terranes such as the Dabie Shan (e.g., Lin et al., 2009), formed by subduction under a continental upper plate. There, Triassic anatexis following (U)HP rock exhumation has been recently documented in migmatites from North Dabie, on the upper-plate side of the (U)HP terrane (Chen et al., 2015).

6.4. (U)HP rock exhumation in eastern PNG

As noted above, the modeled mechanism of (U)HP rock exhumation is largely independent from the nature of the upper plate. Therefore, features similar to those in the Western Alps are also observed in the (U)HP terrane of eastern PNG (e.g., Little et al., 2011; Baldwin et al., 2012). The tectonic domes forming the D'Entrecasteaux Islands are ~30 km in size (Fig. 1), and are exhumed at the rear of a lower-pressure accretionary wedge that developed during northward subduction (Webb et al., 2014) (Fig. 8). While the pressure-time paths of this (U)HP terrane are not yet determined with the same level of detail as for the Western Alps, available petrologic and geochronologic constraints (e.g., Baldwin et al., 2004, 2008; Baldwin and Das, 2015) are consistent with exhumation paths computed by the numerical model (Fig. 8e), indicating fast decompression from mantle depths to the uppermost crust in 3-4 Myr. The gneissic (U)HP domes of the D'Entrecasteaux Islands, unlike those of the Western Alps, are not enveloped by (U)HP metaophiolites, but are tectonically juxtaposed against sedimentary rocks and ophiolites of the upper plate (e.g., Little et al., 2011; Baldwin et al., 2012), in agreement with model predictions. Both in the model and in the D'Entrecasteaux Islands, (U)HP exhumation takes place when rocks of the low-grade frontal wedge, now exposed in the Papuan Peninsula and islands of the southern rifted margin of the Woodlark Basin, were already exhumed (Webb et al., 2014). Similar to the Western Alps, there is a variable rate of upper-plate divergent motion (1.5 to 4 cm/yr) along-strike in the Woodlark Basin, increasing to the east because it is further away from the Woodlark poles of rotation (Petersen and Buck, 2015). However, exhumed (U)HP rocks have only been identified in the D'Entrecasteaux Islands, and the impact of divergence rate on the volume of exhumed (U)HP rocks cannot be ascertained.

6.5. Asthenospheric rise during rifting in eastern PNG

Based on model results, the composition of the upper plate is more relevant for the rifting stage that follows (U)HP rock exhumation (Figs. 4d-e and 8c-d). In eastern PNG, the counterclockwise rotation of the Woodlark plate, which causes upper-plate divergence with resulting (U)HP rock exhumation, also controls the westward propagation of the Woodlark Basin seafloor spreading system (e.g., Webb et al., 2008; Baldwin et al., 2012). When the upper plate is oceanic, numerical models show that deformation is more focused on the lower-plate side of exhumed (U)HP domes (Fig. 8d). This is indeed observed in eastern PNG, where the amount of extension, as recorded in sedimentary basin evolution, is greater in Goodenough Basin (GB in Fig. 1), to the south of the D'Entrecasteaux Islands, than in the Trobriand platform to the north (TP in Fig. 1) (e.g., Fitz and Mann, 2013). The rather thin sedimentary succession of the Goodenough Basin may indicate that tectonic subsidence was partly counterbalanced by the effects of asthenospheric rising. The models indicate that asthenospheric rise during the rifting stage would be particularly important beneath the exhumed (U)HP domes, and asthenospheric material at shallow depths (~20 km) has been imaged beneath the D'Entrecasteaux Islands by analysis of seismic S waves (Abers et al., 2016, their Fig. 7a,b). The modeled thermal structure (see Fig. 8) is confirmed by measured heat-flow showing higher values under the D'Entrecasteaux Islands than in the Goodenough Basin (Martinez et al., 2001). The sharp near-vertical thermal boundary separating the rising asthenosphere from the colder lithospheric mantle of the upper plate (Fig. 8d) is also imaged by a sharp increase in S-wave velocities beneath the Trobriand platform (Jin et al., 2015, their Fig. 11). The low temperatures predicted by numerical modeling in the lithospheric mantle of the upper plate may provide an explanation for the anomalously deep seismic events recorded to the west of the D'Entrecasteaux Island (Abers et al. 2016).

6.6. Exhumation within the subduction channel vs trans-mantle diapirism

The gneissic (U)HP domes of eastern PNG are now exposed directly above the asthenospheric mantle. However, our thermo-mechanical models demonstrate that their exhumation was not the result of "trans-mantle diapirism" (Ellis et al., 2011; Little et al., 2011). Instead, the domes are more likely the result of buoyancy-driven exhumation within the subduction channel, that was triggered, as in the Western Alps, by upper-plate divergent motion that provided accommodation space (Fig. 8). As shown in Fig. 9, continental (U)HP rocks never crossed the crust-mantle boundary during subduction and exhumation. Upper-plate divergence is not only consistent with regional geologic constraints, but allow for the preservation of coesite (Baldwin et al., 2008) and argon retention in phengite in exhumed (U)HP rocks (Baldwin and Das, 2105). In contrast, exhumation mechanisms involving trans-mantle diapirism would not favor preservation of coesite, and would lead to chemical and isotopic resetting of white micas (e.g reset $^{40}Ar/^{39}Ar$ ages in recrystallized muscovite). However, fluids released by dehydration reactions at the slab interface may favor retrogression of (U)HP assemblages during exhumation. Model predictions of focused deformation and partial melting beneath the dome (p in Fig. 8c) are confirmed by GPS data and basaltic volcanism (Fig. 1), and are consistent with S-wave velocity measurements from sites near Quaternary volcanic centers and young plutons of the D'Entrecasteaux Islands (Abers et al., 2016). Notably, partial melting is a late feature of the model evolution, and does not affect the dynamics of (U)HP exhumation (cf. Gordon et al., 2012).

6.7. Role of slab breakoff and comparison with models of slab eduction

The model of (U)HP rock exhumation triggered by upper-plate divergence (Malusà et al., 2011) does not require slab breakoff. When applied to eastern PNG, it has commonalities with published models of subduction inversion (Webb et al., 2008) and slab eduction (Petersen and Buck, 2015). For example, the origin of upper-plate divergent motion is ascribed, in these models, to the onset of subduction along the New Britain trench to the north. However, the eduction model of Petersen and Buck (2015) requires slab breakoff, which is ruled out, at least in the case of the Western Alps, by recent high-resolution tomography models that imaged a continuous European slab (Zhao et al., 2016). The resolution of available tomographic images is much lower in eastern PNG (e.g., Eilon et al., 2015) as compared to the Alps (Zhao et al., 2016). This is likely due to the lower number of available broadband seismic stations (39 vs 527 for the studies quoted above). Therefore, the hypothesis (or the lack) of slab breakoff remains to be tested. On the other hand, the metamorphic field gradients predicted by numerical models of upper-plate divergent motion could be misinterpreted as evidence of slab eduction (e.g., Andersen et al., 1991). Such an interpretation would require a reliable assessment of the relationships between exhumed (U)HP rocks and the slab structure at the time of exhumation, information that is generally not available for pre-Cenozoic (U)HP terranes (Zhao et al., 2017).

7. Summary and conclusions

Thermomechanical models presented here provide support for the hypothesis, first proposed from a geologic perspective, that upper-plate divergence can trigger rapid exhumation of large volumes of (U)HP rocks directly to the Earth's surface, without significant overburden removal via erosional processes. Model results are fully consistent, for a wide range of upper-plate divergence rates, with exhumation paths reconstructed from petrologic and geochronologic data for Cenozoic (U)HP terranes of the Western Alps and eastern PNG. Model tracers reach the Earth's surface rapidly without stalling in the mid-upper crust, and exhumation rates are systematically higher than the divergence rate of the upper plate. The modeled size of exhumed (U)HP domes is consistent with geologic observations, and is invariant for different rates of upper-plate divergent motion. Although the size of exhumed (U)HP domes associated with upper-plate divergent motion are all about the same, major variations are predicted in the deep tectonic structure, because larger amounts of upper-plate divergent motion may allow the exhumation of mantle-wedge serpentinites to shallow depths beneath the domes. The transient rapid temperature increase accompanying the ascent of mantle-wedge material within the subduction channel may be revealed, in exhumed (U)HP rocks, through application of petrology and thermochronology.

During the main stage of (U)HP rock exhumation, the impact of the upper-plate composition is minor, but exhumation is delayed by 1-2 Myr if the upper plate is oceanic. Modeled continental (U)HP domes are enveloped by (U)HP metaophiolites if the upper plate is continental, or tectonically juxtaposed against sedimentary rocks and ophiolites of the upper plate, if it is oceanic. The same relationships are observed in the Alpine and Papuan cases, respectively. The upper plate composition is more relevant during the rifting stage following (U)HP rock exhumation. If the upper plate is continental, deformation is distributed throughout the upper plate. If the upper plate is oceanic, deformation is focused on the lower-plate side of the exhumed (U)HP dome, and asthenospheric rise beneath the dome has the potential to overprint (U)HP mineral assemblages. In the case of protracted upper-plate divergence and/or if the transition to seafloor spreading occurs, the geologic record of (U)HP rock exhumation may be obliterated in a few millions of years.

Model predictions fit a wide range of geologic evidence from the Western Alps, where the geologic record of (U)HP rock exhumation is particularly well preserved, and from eastern PNG, where the tectonics associated with (U)HP rock exhumation are still active. While these terranes have different pre-exhumation histories, their exhumation histories are similar, and (U)HP rock exhumation can be explained as largely controlled by the kinematics of the upper plate. The good fit between model predictions and the geologic record in these (U)HP terranes encourages the application to other (U)HP terranes where the geologic record of exhumation is only partly preserved, and the underlying exhumation mechanisms not fully determined.

Acknowledgments

MM and LZ acknowledge colleagues of the CIFALPS working group for insightful discussions, and Yonghong Shi for illustrating Dabie geology in the field. Funding from the Swiss National Science Foundation - Swiss-AlpArray SINERGIA project CRSII2_154434/1 (to JL), the US National Science Foundation for projects in PNG (to SLB and PGF), and the Thonis endowment (to SLB) is gratefully acknowledged. The manuscript benefited from constructive comments by the Editor Rebecca Bendick and two anonymous reviewers.

REFERENCES

1. Abers, G. A., Eilon, Z., Gaherty, J. B., Jin, G., Kim, Y. H., Obrebski, M., Dieck, C., 2016. Southeast Papuan crustal tectonics: Imaging extension and buoyancy of an active rift. Journal of Geophysical Research: Solid Earth 121(2), 951-971.
2. Andersen, T. B., Jamtveit, B., Dewey, J. F., Swensson, E., 1991. Subduction and eduction of continental crust: major mechanisms during continent-continent collision and orogenic extensional collapse, a model based on the south Norwegian Caledonides. Terra Nova 3(3), 303-310.
3. Baldwin, S. L., Das, J. P., 2015. Atmospheric Ar and Ne returned from mantle depths to the Earth’s surface by forearc recycling. Proceedings of the National Academy of Sciences 112(46), 14174-14179.
4. Baldwin, S. L., Monteleone, B. D., Webb, L. E., Fitzgerald, P. G., Grove, M., Hill, E. J., 2004. Pliocene eclogite exhumation at plate tectonic rates in eastern Papua New Guinea. Nature 431(7006), 263-267.
5. Baldwin, S. L., Webb, L. E., Monteleone, B. D., 2008. Late Miocene coesite-eclogite exhumed in the Woodlark Rift. Geology 36(9), 735-738.
6. Baldwin, S. L., Fitzgerald, P. G., Webb, L. E., 2012. Tectonics of the New Guinea region. Annual Review of Earth and Planetary Sciences 40, 495–520.
7. Beaumont, C., Jamieson, R. A., Nguyen, M. H., Lee, B., 2001. Himalayan tectonics explained by extrusion of a low-viscosity crustal channel coupled to focused surface denudation. Nature 414(6865), 738-742.
8. Blake, M. C., Jayko, A. S., 1990. Uplift of very high pressure rocks in the western Alps:

evidence for structural attenuation along low-angle faults. Mémoires de la Société géologique de France 156, 237-246.

9. Brun, J.P., Faccenna, C., 2008. Exhumation of high-pressure rocks driven by slab rollback. Earth and Planetary Science Letters 272, 1-7.

10. Burov, E., Cloetingh, S. (1997). Erosion and rift dynamics: new thermomechanical aspects of post-rift evolution of extensional basins. Earth and Planetary Science Letters 150, 7-26.

11. Butler, J. P., Beaumont, C., Jamieson, R. A., 2013. The Alps 1: A working geodynamic model for burial and exhumation of (ultra) high-pressure rocks in Alpine-type orogens. Earth and Planetary Science Letters 377, 114-131.

12. Chen, R. X., Ding, B., Zheng, Y. F., Hu, Z., 2015. Multiple episodes of anatexis in a collisional orogen: Zircon evidence from migmatite in the Dabie orogen. Lithos 212, 247-265.

13. Chopin, C., 2003. Ultrahigh-pressure metamorphism: tracing continental crust into the mantle. Earth and Planetary Science Letters 212(1), 1-14.

14. Compagnoni, R., 2003. HP metamorphic belt of the western Alps. Episodes 26(3), 200-204.

15. Compagnoni, R., Rolfo, F., 2003. UHPM units in the Western Alps. Ultrahigh pressure metamorphism 5, 13-49.

16. Crameri, F., Tackley, P. J., Meilick, I., Gerya, T. V., Kaus, B. J. P., 2012. A free plate surface and weak oceanic crust produce single - sided subduction on Earth. Geophysical Research Letters 39(3).

17. Dewey, J., Helman, M., Knott, S., Turco, E., Hutton, D. 1989. Kinematics of the western Mediterranean. Geological Society, London, Special Publications 45, 265-283.

18. Ducea, M. N., 2016. Research Focus: Understanding continental subduction: A work in progress. Geology 44(3), 239-240.

19. Eilon, Z., Abers, G. A., Gaherty, J. B., Jin, G., 2015. Imaging continental breakup using teleseismic body waves: the Woodlark Rift, Papua New Guinea. Geochemistry, Geophysics, Geosystems 16, 2529-2548.

20. Ellis, S. M., Little, T. A., Wallace, L. M., Hacker, B. R., Buiter, S. J. H., 2011. Feedback between rifting and diapirism can exhume ultrahigh-pressure rocks. Earth and Planetary Science Letters 311(3), 427-438.

21. Fitz, G., Mann, P., 2013. Tectonic uplift mechanism of the Goodenough and Fergusson Island gneiss domes, eastern Papua New Guinea: Constraints from seismic reflection and well data. Geochemistry, Geophysics, Geosystems 14(10), 3969-3995.

22. Gerya, T. V., Yuen, D. A., 2003a. Rayleigh–Taylor instabilities from hydration and melting propel ‘cold plumes’ at subduction zones. Earth and Planetary Science Letters 212(1), 47-62.

23. Gerya, T. V., Yuen, D. A., 2003b. Characteristics-based marker-in-cell method with conservative finite-differences schemes for modeling geological flows with strongly variable transport properties. Physics of the Earth and Planetary Interiors 140(4), 293-318.

24. Gordon, S.M., Little, T.A., Hacker, B.R., Bowring, S.A., Korchinski, M., Baldwin, S.L., Kylander-Clark, A.R.C., 2012. Multi-stage exhumation of young UHP–HP rocks: Timescales of melt crystallization in the D’Entrecasteaux Islands, southeastern Papua New Guinea. Earth and Planetary Science Letters 351-352, 237-246.

25. Groppo, C., Beltrando, M., Compagnoni, R., 2009. The P–T path of the ultra-high pressure Lago di Cignana and adjoining high-pressure meta-ophiolitic units: insights into the evolution of the subducting Tethyan slab. Journal of Metamorphic Geology 27(3), 207-231.

26. Guillot, S., Hattori, K., Agard, P., Schwartz, S., Vidal, O., 2009. Exhumation processes in oceanic and continental subduction contexts: a review. In Subduction Zone Geodynamics (pp. 175-205). Springer, Berlin, Heidelberg.

27. Hacker, B. R., Gerya, T. V., 2013. Paradigms, new and old, for ultrahigh-pressure tectonism. Tectonophysics 603, 79-88.

28. Hill, E. J., 1994. Geometry and kinematics of shear zones formed during continental extension in eastern Papua New Guinea. Journal of Structural Geology 16(8), 1093-1105.

29. Jin, G., Gaherty, J. B., Abers, G. A., Kim, Y., Eilon, Z., Buck, W. R., 2015. Crust and upper mantle structure associated with extension in the Woodlark Rift, Papua New Guinea from Rayleigh-wave tomography. Geochemistry Geophysics Geosystems 16(11), 3808-3824.

30. Li, Z. H., Xu, Z. Q., Gerya, T. V., 2011. Flat versus steep subduction: Contrasting modes for the formation and exhumation of high-to ultrahigh-pressure rocks in continental collision zones. Earth and Planetary Science Letters 301(1), 65-77.

31. Liao, J., Gerya, T., 2014. Influence of lithospheric mantle stratification on craton extension: Insight from two-dimensional thermo-mechanical modeling. Tectonophysics 631, 50-64.

32. Lin, W., Shi, Y., Wang, Q., 2009. Exhumation tectonics of the HP-UHP orogenic belt in Eastern China: New structural–petrological insights from the Tongcheng massif, Eastern Dabieshan. Lithos 109(3), 285-303.

33. Little, T. A., Hacker, B. R., Gordon, S. M., Baldwin, S. L., Fitzgerald, P. G., Ellis, S., Korchinski, M., 2011. Diapiric exhumation of Earth's youngest (UHP) eclogites in the gneiss domes of the D'Entrecasteaux Islands, Papua New Guinea. Tectonophysics 510(1), 39-68.

34. Malusà, M. G., Polino, R., Zattin, M., Bigazzi, G., Martin, S., Piana, F., 2005. Miocene to Present differential exhumation in the Western Alps: Insights from fission track thermochronology. Tectonics 24(3).

35. Malusà, M. G., Faccenna, C., Garzanti, E., Polino, R., 2011. Divergence in subduction zones and exhumation of high pressure rocks (Eocene Western Alps). Earth and Planetary Science Letters 310(1), 21-32.

36. Malusà, M. G., Faccenna, C., Baldwin, S. L., Fitzgerald, P. G., Rossetti, F., Balestrieri, M. L., Danisik, M., Ellero, A., Ottria, G., Piromallo, C., 2015. Contrasting styles of (U) HP rock exhumation along the Cenozoic Adria-Europe plate boundary (Western Alps, Calabria, Corsica). Geochemistry Geophysics Geosystems 16(6), 1786-1824.

37. Malusà, M. G., Zhao, L., Eva, E., Solarino, S., Paul, A., Guillot, S., Schwartz, S., Dumont, T., Aubert, C., Salimbeni, S., Pondrelli, S., Wang, Q., Zhu, R., 2017. Earthquakes in the western Alpine mantle wedge. Gondwana Research 44, 89-95.

38. Martinez, F., Goodliffe, A. M., Taylor, B., 2001. Metamorphic core complex formation by density inversion and lower-crust extrusion. Nature 411(6840), 930-934.

39. Nikolaeva, K., Gerya, T. V., Marques, F. O., 2010. Subduction initiation at passive margins: numerical modeling. Journal of Geophysical Research: Solid Earth, 115(B3).

40. Petersen, K. D., Buck, W. R., 2015. Eduction, extension, and exhumation of ultrahigh-pressure rocks in metamorphic core complexes due to subduction initiation. Geochemistry Geophysics Geosystems 16(8), 2564-2581.

41. Roecker, S. W., 1982. Velocity structure of the Pamir-Hindu Kush Region: Possible evidence of subducted crust. Journal of Geophysical Research: Solid Earth 87(B2), 945-959.

42. Rubatto, D., Hermann, J., 2001. Exhumation as fast as subduction? Geology 29(1), 3-6.

43. Schwartz, S., Lardeaux, J. M., Guillot, S., Tricart, P., 2000. Diversité du métamorphisme éclogitique dans le massif ophiolitique du Monviso (Alpes occidentales, Italie). Geodinamica Acta, 13(2-3) 169-188.

44. Solarino, S., Malusà, M.G., Eva, E., Guillot, S., Paul, A., Schwartz, S., Zhao, L., Aubert, C., Dumont, T., Pondrelli, S., Salimbeni, S., Wang, Q., Xu, X., Zheng., T., Zhu, R., 2018. Mantle wedge exhumation beneath the Dora-Maira (U)HP dome unravelled by local earthquake tomography. Lithos 296-299, 623-636.

45. Webb, L. E., Baldwin, S. L., Little, T. A., Fitzgerald, P. G., 2008. Can microplate rotation drive subduction inversion?. Geology 36(10), 823-826.

46. Webb, L. E., Baldwin, S. L., Fitzgerald, P. G., 2014. The Early-Middle Miocene subduction complex of the Louisiade Archipelago, southern margin of the Woodlark Rift. Geochemistry Geophysics Geosystems 15(10), 4024-4046.

47. Yamato, P., Burov, E., Agard, P., Le Pourhiet, L., Jolivet, L., 2008. HP-UHP exhumation during slow continental subduction: Self-consistent thermodynamically and thermomechanically coupled model with application to the Western Alps. Earth and Planetary Science Letters 271(1), 63-74.

48. Zhao, L., Paul, A., Guillot, S., Solarino, S., Malusà, M.G., Zheng, T., Aubert, C., Salimbeni, S., Dumont, T., Schwartz, S., Zhu, R., Wang, Q., 2015. First seismic evidence for continental subduction beneath the Western Alps. Geology 43, 815-818.

49. Zhao, L., Paul, A., Malusà, M.G., Xu, X., Zheng, T., Solarino, S., Guillot, S., Schwartz, S., Dumont, T., Salimbeni, S., Aubert, C., Pondrelli, S., Wang, Q., Zhu, R., 2016. Continuity of the Alpine slab unraveled by high-resolution P wave tomography. Journal of Geophysical Research: Solid Earth 121, 8720–8737.

50. Zhao, L., Xu, X., Malusà, M. G., 2017. Seismic probing of continental subduction zones. Journal of Asian Earth Sciences 145, 37-45.

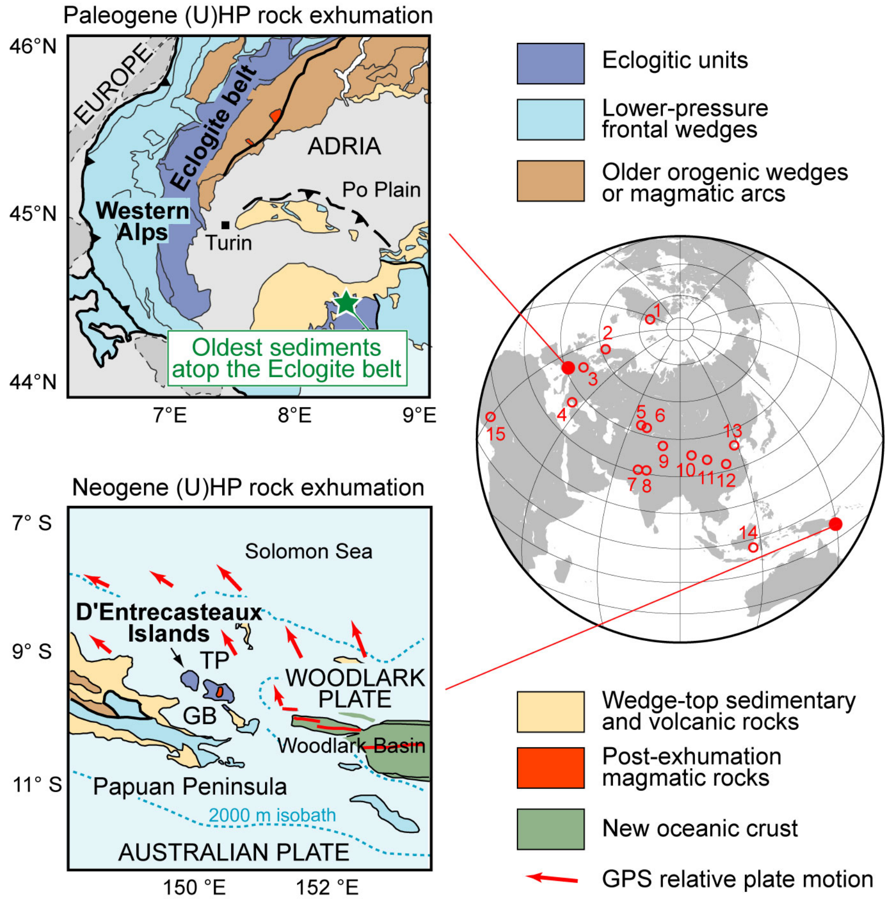

Fig. 1. On the left, tectonic sketch maps of the (U)HP terranes of the Western Alps (after Malusà et al., 2011) and eastern PNG (after Baldwin et al., 2008); GB, Goodenough Basin; TP, Trobriand platform. On the right, location of other UHP occurrences in continental units: 1, East Greenland; 2, Western Gneiss Region; 3, Bohemia; 4, Rhodope; 5, Chara; 6, Kokchetav; 7, Kaghan; 8, Tso Morari; 9, West Tianshan; 10, North Qaidam; 11, Quinling; 12, Dabie Shan; 13, Sulu; 14, Central Sulawesi; 15, Gourma (after Guillot et al., 2009).

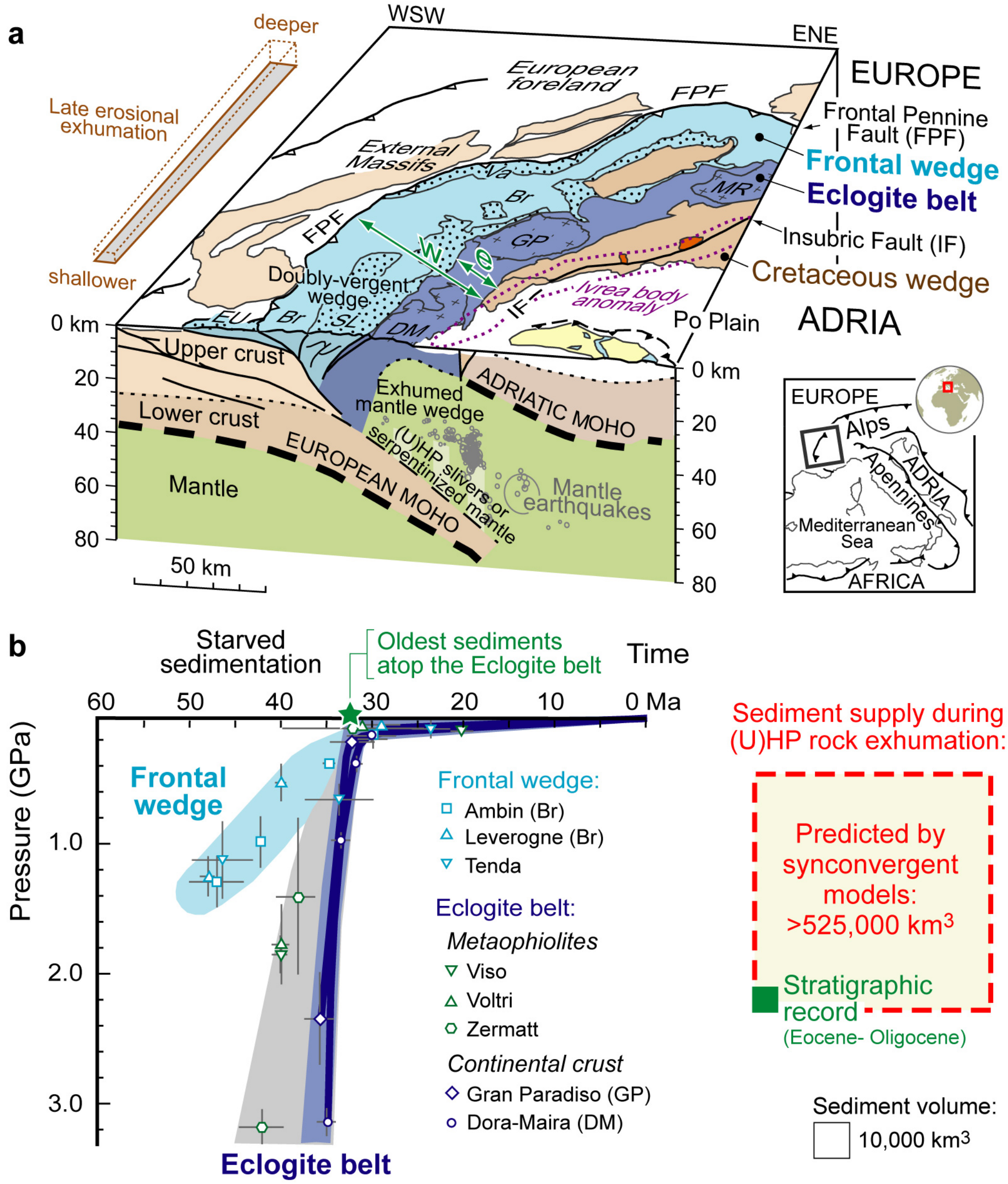

Fig. 2. Geologic constraints from the Western Alps. **a,** Main tectonic structures (after Zhao et al., 2015; Malusà et al., 2017; Solarino et al., 2018) and trend of late erosional exhumation (after Malusà et al., 2005); green arrows indicate the width of exhumed eclogitic units (e) compared to the total width of the metamorphic belt (w). **b,** Pressure-time exhumation path of continental units from the Eclogite belt and the Frontal wedge (after Malusà et al., 2011), and sediment supply predicted by synconvergent exhumation models compared to the stratigraphic record (Malusà et al., 2015). Acronyms: Br, Briançonnais; DM, Dora-Maira; EU, Embrunais-Ubaye; FPF, Frontal Pennine Fault; GP, Gran Paradiso; IF, Insubric Fault; MR, Monte Rosa; SL, Schistes lustrés; Va, Valaisan.

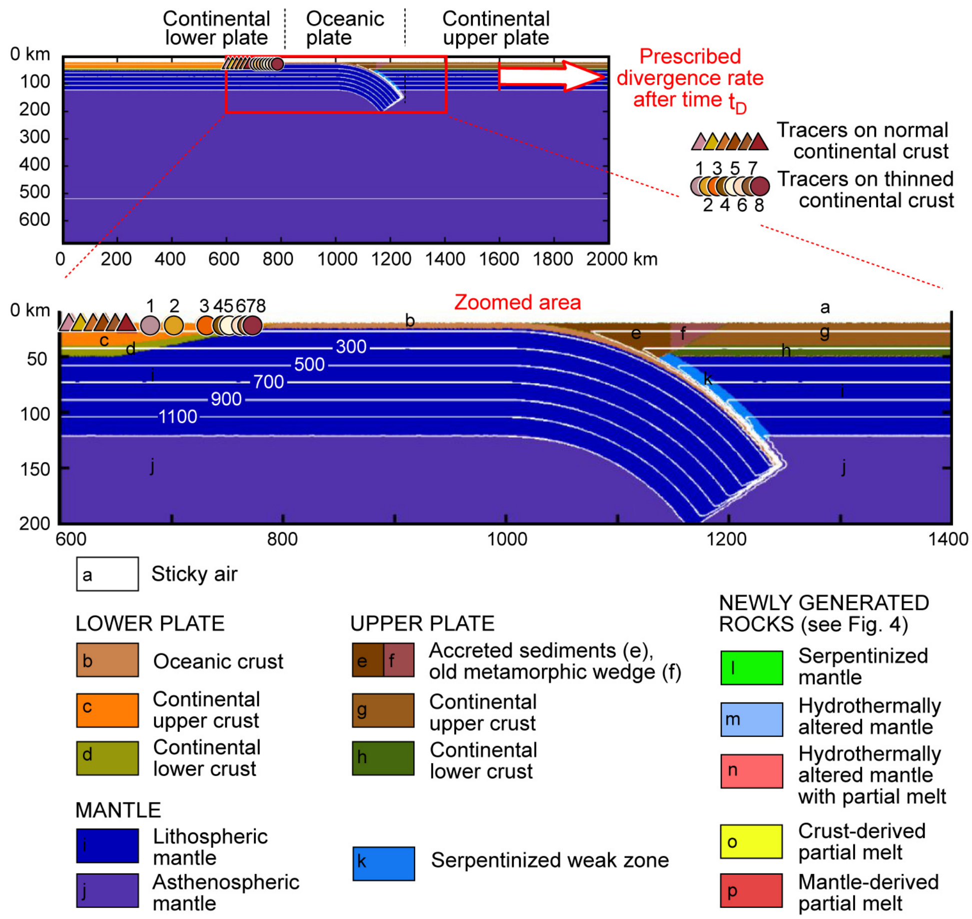

Fig. 3. Model setup assuming a continental upper plate. White lines are isotherms (°C), numbers 1 to 8 indicate tracers on thinned continental crust, t_D indicates the onset of upper-plate divergent motion. The initial and boundary conditions associated with this model setup are relevant for the Western Alps.

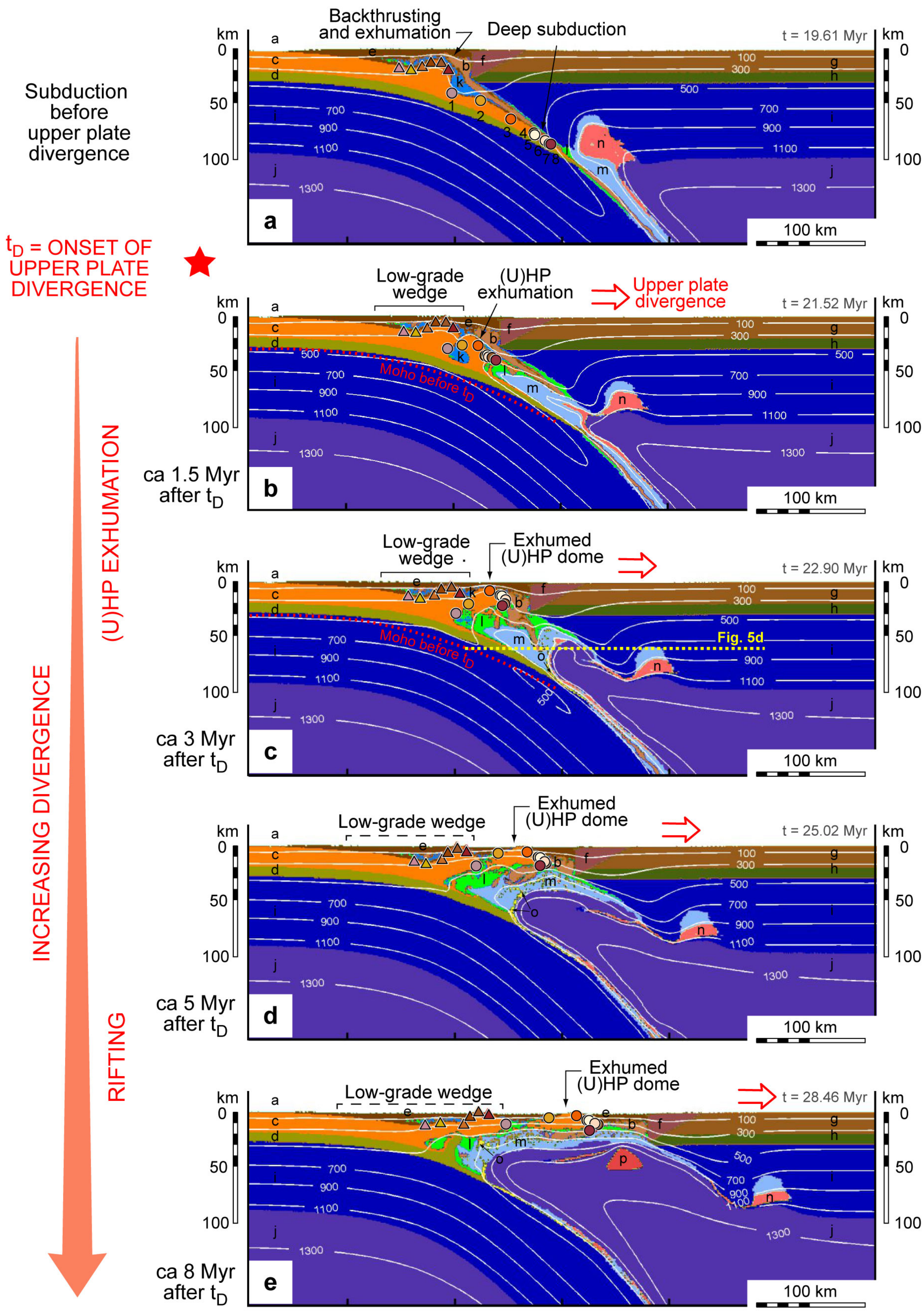

Fig. 4. Numerical model evolution before (a) and after (b-e) the onset of upper-plate divergent motion. The prescribed divergence rate is 2 cm/yr (same keys as in Fig. 3).

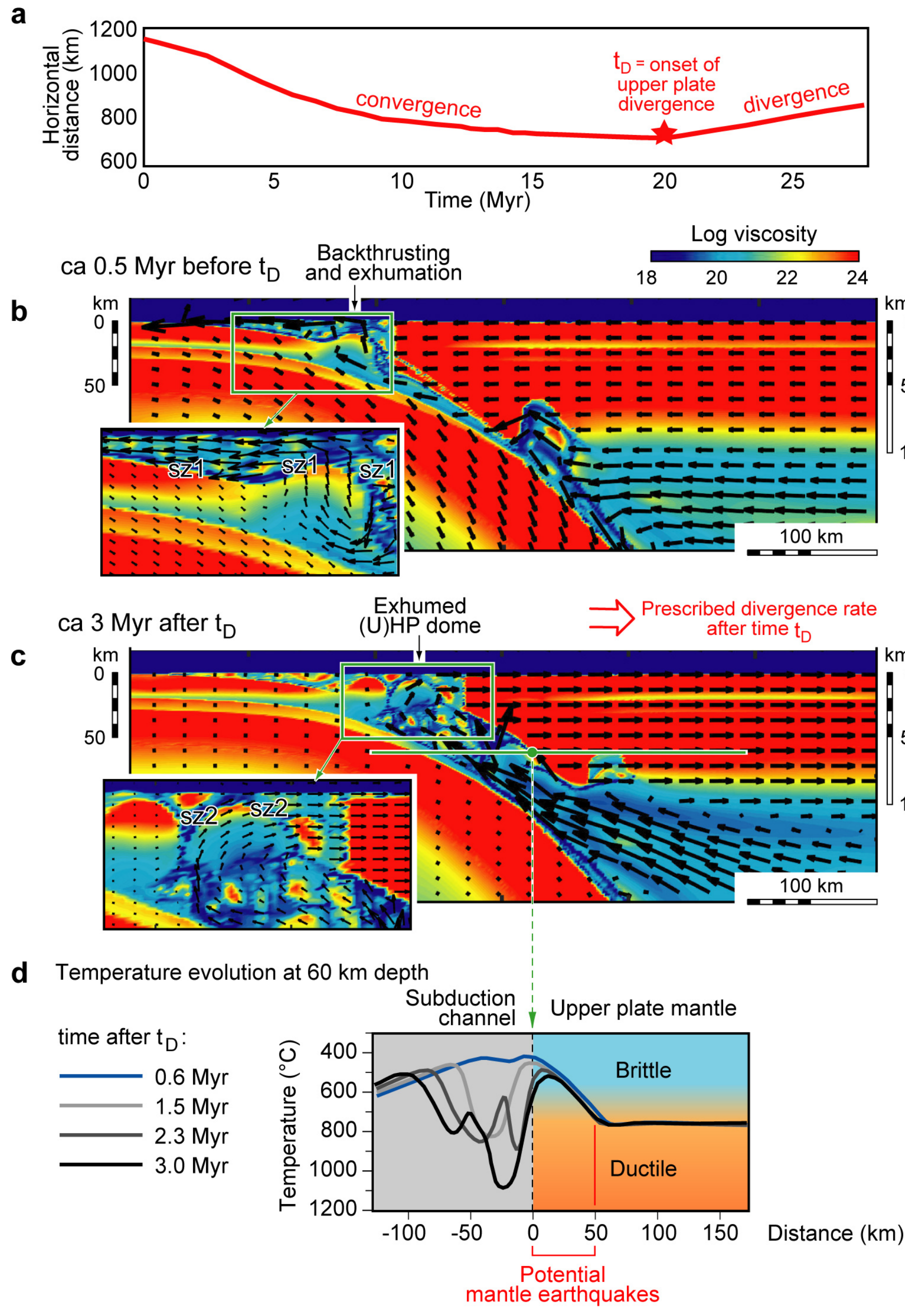

Fig. 5. Dynamic evolution before and after the onset of upper-plate divergence. **a,** Motion of the upper plate during subduction and collision; **b,** Viscosity and velocity field (shown by arrows) before the onset of upper-plate divergent motion; in the inset, note the opposite-dipping shear zones (sz1, in blue) of the frontal wedge (the associated strain-rate plot is in supplementary Fig. S1); **c,** Viscosity and velocity field 3 Myr after the onset of upper-plate divergent motion (prescribed divergent rate = 2 cm/yr); in the inset, note the shear zones (sz2, in blue) on top of the tectonic dome (the associated strain-rate plot is in supplementary Fig. S1); **d,** Temperature evolution during upper-plate divergent motion in the subduction channel and adjoining upper-plate mantle (60 km depth).

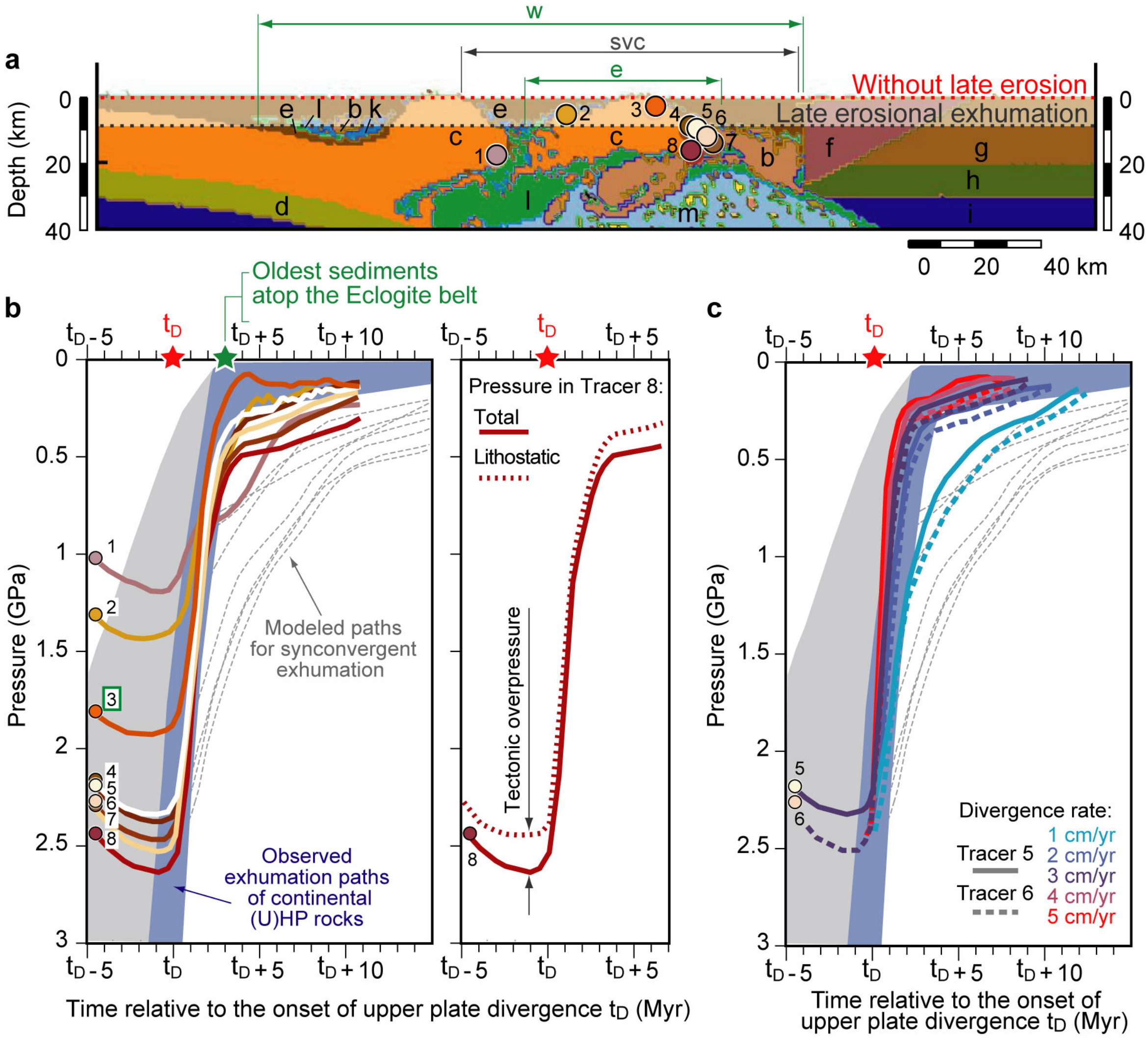

Fig. 6. Modeled pressure-time exhumation paths during upper-plate divergent motion. **a,** Snapshot from Fig. 4d showing composition and structure of exhumed rocks, potential impact of late erosion, and final position of tracers 1 to 8 (keys as in Fig. 3); green arrows indicate the width of exhumed eclogitic units (e) and the width of the whole metamorphic belt (w); the black arrow (svc) indicates the section considered for computation of sediment volume (see Fig. 7b); **b,** On the left, pressure-time exhumation paths of tracers 1 to 8 (divergence rate = 2 cm/yr) compared with modeled paths for synconvergent exhumation (after Butler et al., 2013) and observed exhumation paths of continental (U)HP rocks in the Western Alps (shaded blue). Note the timing of final exhumation of tracer 3, which is consistent with observed early Oligocene sedimentation atop the Eclogite belt (green star, see also Fig. 1). On the right, lithostatic vs total pressure (including tectonic overpressure) recorded by tracer 8. **c,** Pressure-time exhumation paths recorded by tracers 5 (continuous line) and 6 (dashed lines) for different divergent rates prescribed after time t_D.

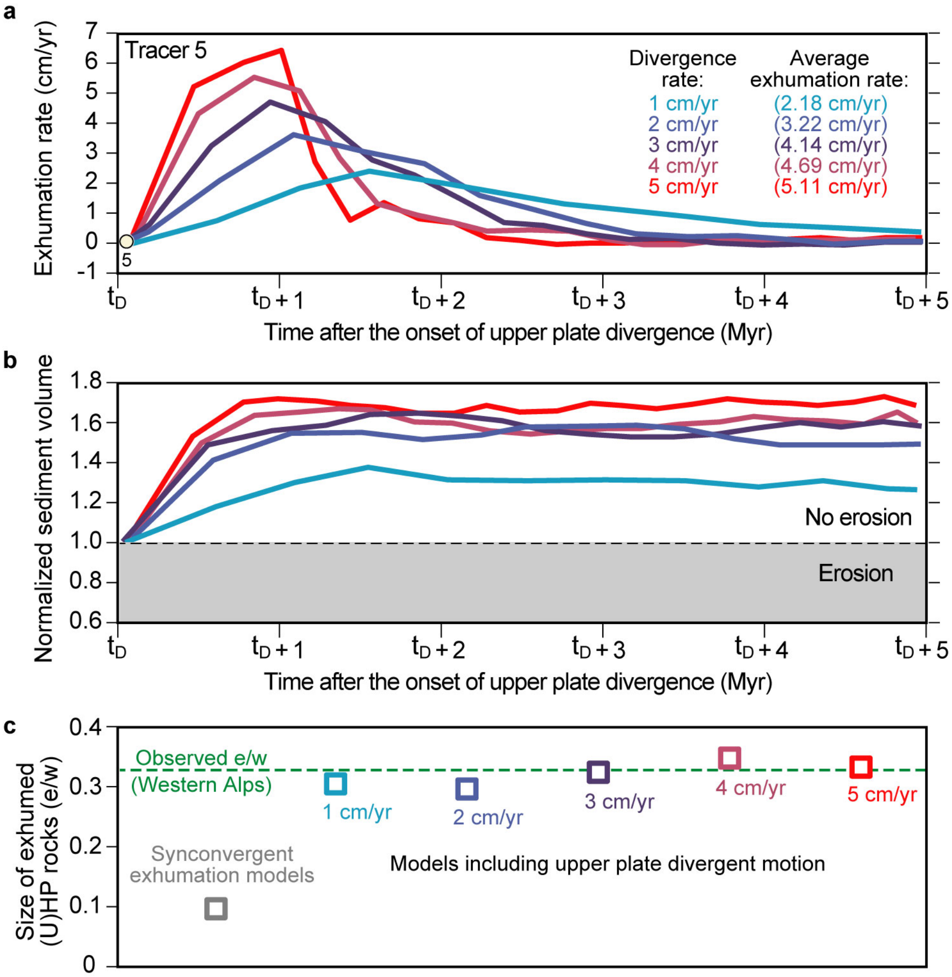

Fig. 7. Impact of divergence rate on exhumation rate and size, and on sediment production. **a,** Exhumation rates recorded by tracer 5 for different divergence rates after the onset of upper-plate divergent motion; **b,** Sediment volume produced during upper-plate divergent motion, normalized to the initial volume calculated at time t_D along section svc in Fig. 6a; **c,** Normalized size of exhumed (U)HP domes for different divergence rates, and comparison with the e/w ratios observed in the Western Alps (green line) and predicted by synconvergent exhumation models (Butler et al., 2013).

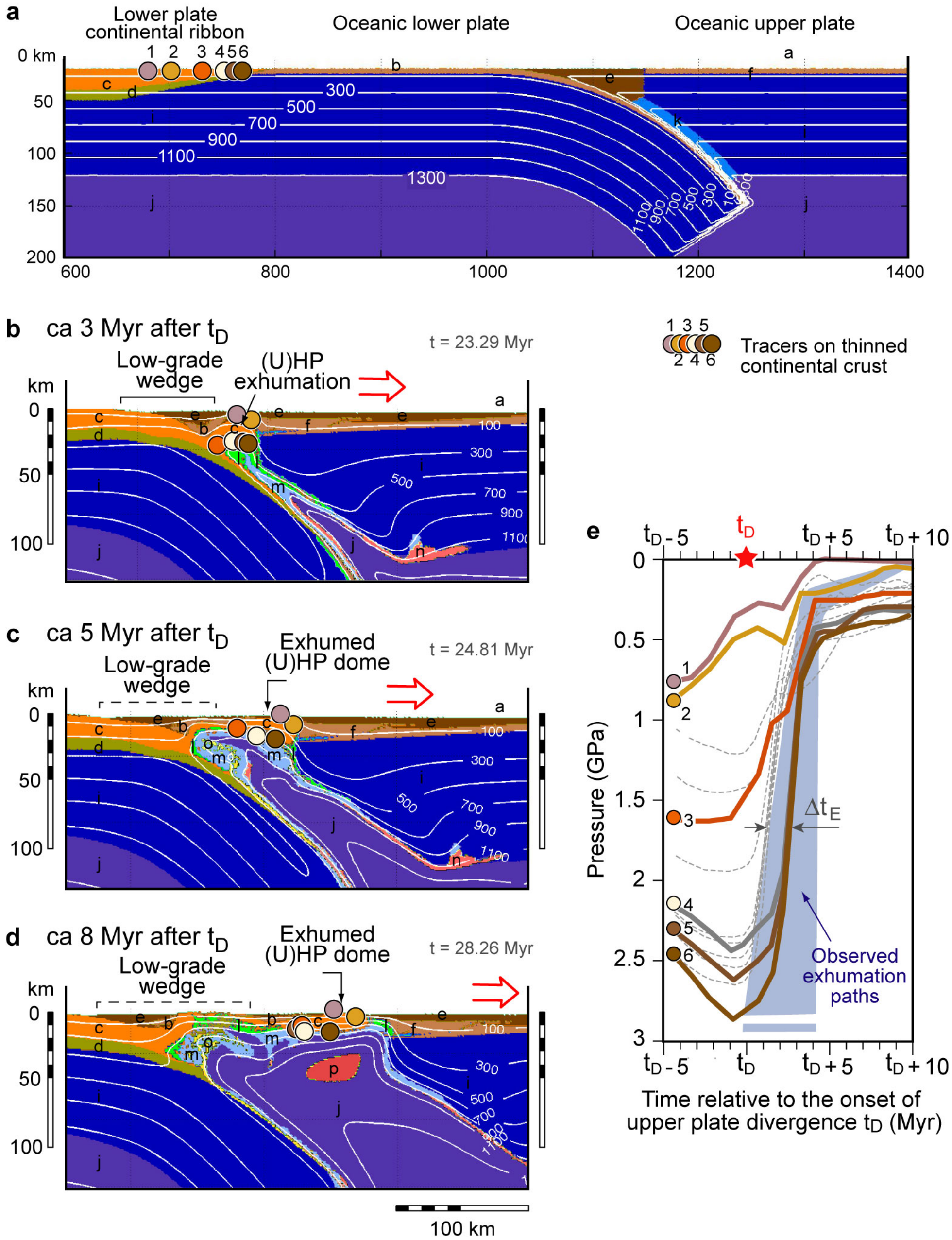

Fig. 8. Numerical model evolution assuming an oceanic upper plate (same keys as in Fig. 3, apart from f that indicates the oceanic crust of the upper plate). **a,** model setup (prescribed divergence rate = 2 cm/yr); **b-d,** snapshots at 3 My, 5 Myr and 8 Myr after the onset of upper-plate divergent motion; **e,** Pressure-time exhumation paths of tracers 1 to 6, the dashed grey lines indicate the exhumation paths assuming a continental upper plate (Fig. 6b), Δt_E indicates the exhumation time delay compared to the model of Fig. 4. The initial and boundary conditions associated with this model are relevant for the eastern Papuan (U)HP terrane (observed exhumation paths based on Fitz and Mann, 2013; Baldwin and Das, 2015).

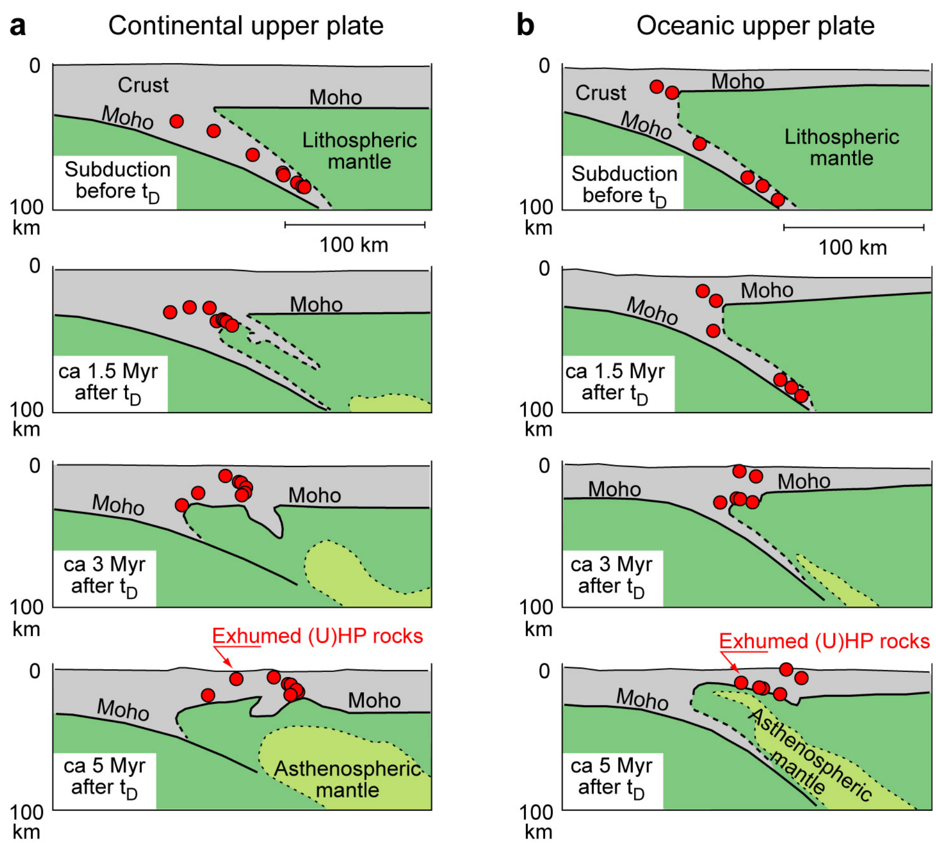

Fig. 9. Modeled relationships between continental (U)HP rocks (red dots) and the Moho (in black), assuming a continental (a) or an oceanic (b) upper plate. In both cases, (U)HP rocks may interact with mantle rocks during subduction and exhumation, but never cross the Moho.